

2018年度 公益財団法人日本台湾交流協会フェロシップ事業成果報告書  
(自然科学分野)

以三維穿透式電子顯微鏡技術解析嵌段共聚合物之圓球堆積結構

陳莉婷  
国立清華大学  
招聘期間 (2018年7月1日～8月29日)  
2018年  
公益財団法人日本台湾交流協会

2018 年度 日本台灣交流協會招聘活動 (自然科學相關領域)

研究成果報告書

研究主題：

以三維穿透式電子顯微鏡技術解析嵌段共聚合物之圓球堆積結構(中文)

三次元電子顯微鏡法によるブロック共重合体が自己組織化する球状ナノ構造の解明(日文)

報告人：陳莉婷

所屬單位：國立清華大學化學工程系

研究期間：2018 年 7 月 1 日至 2018 年 8 月 29 日

## Introduction

Block copolymers constitute an important family of nanostructured materials with great potentials of applications in various areas including photonics, opto-electronics and biomedicines. The great feature of block copolymer lies in its ability to self-assemble to form a variety of periodic nanostructures governed largely by the composition of the constituent blocks. When the composition is highly asymmetric, the minority blocks self-assemble to form spherical microdomains dispersed in the matrix phase composed of the majority blocks; the spherical domains thus formed have been found to pack almost exclusively in body-centered cubic (BCC) lattice.<sup>1-3</sup> In addition to BCC packing, closely packed spheres (CPS) in face-centered cubic (FCC) or hexagonal closely packed (HCP) lattices have been predicted to exist over a very narrow window in the phase diagram.<sup>4</sup>

Block copolymer mesophase may also be tailored by blending the copolymer with the corresponding homopolymer, as the amount of homopolymer solubilized uniformly into the microdomains under the wet-brush condition tunes the overall composition of the constituents. The self-consistent field calculation showed that the composition window of the CPS phase in block copolymer/homopolymer blend became broader than that in the neat copolymer.<sup>5,6</sup> In a previous study, our laboratory has revealed the existence of FCC-packed poly(ethylene oxide) (PEO) spheres in a blend of a symmetric poly(ethylene oxide)-*block*-poly(1,4-butadiene) (PEO-*b*-PB) and a PB homopolymer (h-PB). This system was shown to undergo an order-order transition (OOT) from BCC to FCC phase on heating. Moreover, the OOT occurred via a precursor-driven mechanism, where the OOT became inaccessible once the system did not contain the BCC or FCC precursor prior to the transition.<sup>7,8</sup>

In my recent analysis of the small angle X-ray scattering (SAXS) profiles of the FCC-packed spheres of PEO-*b*-PB/h-PB blends, an interesting feature of the scattering pattern was identified, as shown in Figure 1. In the experimentally observed SAXS profile, (111) and (220) peaks of the FCC lattice were sharp, but (200) peak was broad. The peak broadening may arise from the limited grain size and/or the lattice distortion which are accounted for by the paracrystalline model. Therefore, we used paracrystalline model to calculate the SAXS profile of the FCC-packed spheres, as shown by the blue curve in Figure 1. It can be seen that, if we wanted to broaden (200) peak to match the experimentally observed peak width by reducing the grain size or

increasing the lattice distortion, (111) and (220) peaks also broadened simultaneously. Hence, the features of the experimental SAXS profile of the FCC-packed spheres could not be described by the paracrystalline model.

The observed SAXS pattern may be ascribed to the presence of stacking faults in the FCC lattice. It is known that FCC lattice is constructed by the stacking of the hexagonal closely-packed layers of the spherical microdomains in the ABCABC... sequence along (111) direction. It is likely that the stacking of the hexagonal closely packed layers did not completely follow such a sequence due to kinetic reason, such that a significant amount of stacking fault existed in the FCC phase. In this case, the ABC stacking sequence was intervened with some “non-ABC” sequence (e.g. ABCABCACBABCACABC...). The red scattering curve in Figure 1 was calculated by assuming the stacking sequence of ABCABCABCBCBACABCACACBAC. It can be seen that the consideration of the stacking fault reproduced the features of the observed SAXS profile well, as the calculated profile displayed sharp (111) and (220) peaks and broad (200) peak.

Since the analysis of the SAXS profile may not be unambiguous, we attempt to visualize the stacking sequence of the spherical microdomains in three dimensions by transmission electron microtomography (TEMT) to verify the existence of stacking fault in the FCC phase of the soft spheres. I plan to visit Professor Hiroshi Jinnai’s laboratory at the Institute of Multidisciplinary Research for Advanced Materials (IMRAM) at Tohoku University for two months to perform the TEMT experiment. Prof. Jinnai is one of the world-leading scientists in the field of TEMT in the world. His laboratory is equipped with the most advanced TEM facility for resolving nano-scale structures of soft materials in 3D. If I am granted the scholarship, I plan to learn all the skills relevant to TEMT in Prof. Jinnai’s laboratory, including sample preparation, TEM facility operation, and image analysis and construction. This technique will be applied to resolve the stacking fault of the sphere-forming PEO-b-PB/h-PB blend systems. By combining TEMT and SAXS results, we shall be able to yield the unprecedented details and insights into the self-assembly of the spherical domains of block copolymers. Our work is important in the sense that the stacking fault of the micelles, which is still poorly understood so far for block copolymer systems, is expected to influence the properties of the copolymer strongly.

From the perspective of my career, I believe that combining the TEMT techniques of Prof. Jinnai’s group and the scattering techniques I am

familiar with will allow me to explore my current project in a vigorous way. Besides broadening my horizon by doing TEMT experiments with Prof. Jinnai's group, I would like to share the works from our group in Taiwan with them. I believe there will be valuable suggestions for me to bring back to my labmates.

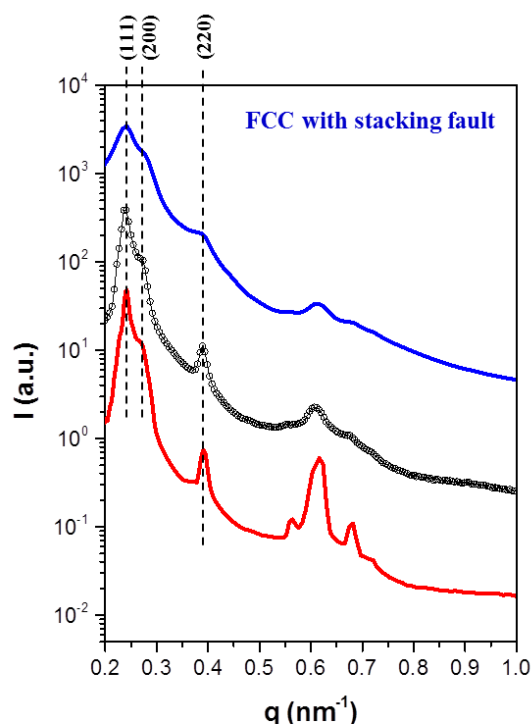


Figure 1. SAXS profiles of  $\text{PEO}_{7.5\text{k}}\text{-}b\text{-}\text{PB}_{5.5\text{k}}$  /  $\text{h-PB}_{1\text{k}}$  blend with PEO volume fraction,  $f_{\text{PEO}} = 0.17$ . The black curve is the experimentally observed profile; the blue curve is the scattering profile calculated by the paracrystalline model, and the red curve was calculated by considering the stacking fault with the stacking sequence of the hexagonal closely packed layers of **ABCABCBCBACABCACACBAC**

### Schedule planning

This proposal proposes the detailed study of the self-assembly of spherical micelles formed by block copolymers by means of TEMT techniques, with particular emphasis on resolving the stacking fault of the spherical domains in the CPS phase of PEO-*b*-PB systems. I plan to visit Professor Hiroshi Jinnai's laboratory at the Institute of Multidisciplinary Research for Advanced Materials (IMRAM) at Tohoku University for two months to perform the TEMT experiment. The following tasks associated with the TEMT study will be performed:

- (1) Sample preparation.
- (2) TEM facility operation for image collection.
- (3) Image analysis and construction.

At the beginning, I will choose a test sample, ro254, which is easier to prepare to learn TEM technique. Next, I will use this technique to characterize the morphology of both neat PEO-*b*-PB and PEO-*b*-PB/h-PB blends. The structures will be resolved as a function of the composition and the history of sample preparation as well as thermal treatment. Prior to my visit to Prof. Jinnai's laboratory, I will first collect the SAXS profiles of the samples using the SAXS beamlines at the National Synchrotron Radiation Research Center (NSRRC) in Taiwan. The structural details will then be established through the conjunction of SAXS and TEM results. By combining these two techniques, we will be able to yield the unprecedented details and insights into the self-assembly of the spherical domains of block copolymers. The results will make a significant contribution to the fundamental studies of block copolymers and shall be published in high-impact journals.

The following table summarizes the schedule of the proposed works:

list of work	1 <sup>st</sup> week	2 <sup>nd</sup> week	3 <sup>rd</sup> week	4 <sup>th</sup> week	5 <sup>th</sup> week	6 <sup>th</sup> week	7 <sup>th</sup> week	8 <sup>th</sup> week
Sample preparation (ultramicrotomy) (a) Ultrathin section (b) Staining								
Image collection (a) Tilt-series images recording								
Image analysis (a) 3D reconstruction Alignment of the data stack Reconstruction by back-projection (b) 3D visualization								

## Experimental section

### (1) Information of the test sample (ro254)

Figure 2 is the structure formula of ro254. The number average molecular weight ( $M_n$ ) of ro254 is 7,900, with the weight percentage of PS and PMSC3OH block of 38% and 62%, respectively. Figure 3 is

SAXS profile of ro254. According to the SAXS profile, the morphology at high temperature may be hexagonal-perforate lamellar (HPL) and ABAB-stacking; however, it may be HPL and ABCABC-stacking at low temperature. In my study, I will choose ro254 with ABAB-stacking (the sample is quenched from 200°C) as the test sample.

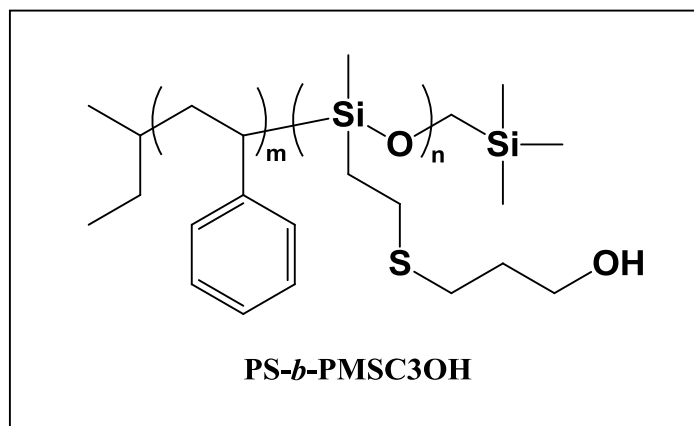


Figure 2. Structure formula of ro254. The repeat unit of *m* is PS block; the repeat unit of *n* is PMSC3OH block.

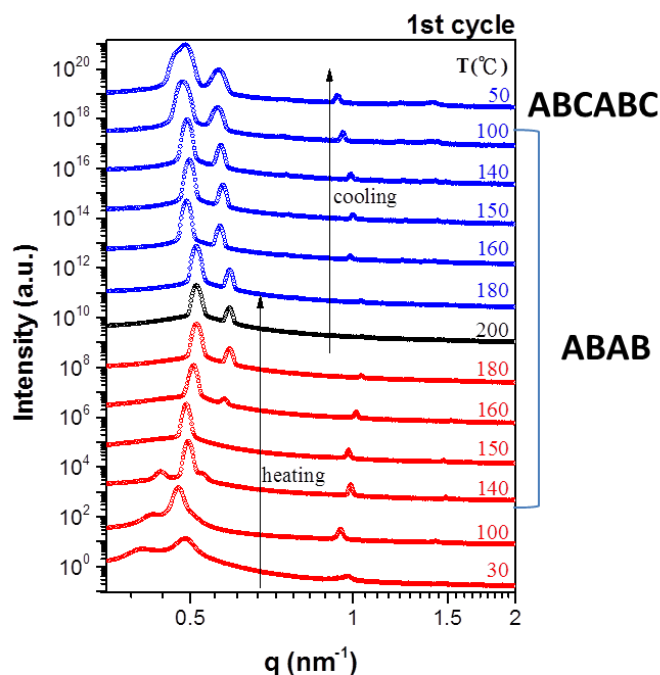


Figure 3. SAXS profile of ro254. In the heating process (red curves) from 140°C to 200°C and then cooling (blue curves) to 100°C, the morphology is ABAB-stacking; at the beginning of heating and at the end of cooling the morphology is ABCABC-stacking.

## (2) Information of PEO-*b*-PB/h-PB

Figure 4 is the structure formula of PEO-*b*-PB. The PEO-*b*-PB with the  $M_n$  of PEO and PB block of  $7.5 \times 10^3$  and  $5.5 \times 10^3$  g/mol, respectively, was acquired from Polymer Source, Inc. Its polydispersity index ( $M_w/M_n$ ) was 1.04. The 1,4-addition h-PB with  $M_n = 1.0 \times 10^3$  g/mol was also obtained from Polymer Source, Inc. The blends with the overall volume fractions of PEO ( $f_{PEO}$ ) of 0.17 were prepared by solvent casting. The PEO-*b*-PB and the homopolymers were first dissolved in toluene at room temperature followed by drying in vacuo at 60 °C for 4 hours to obtain the solvent-cast bends.

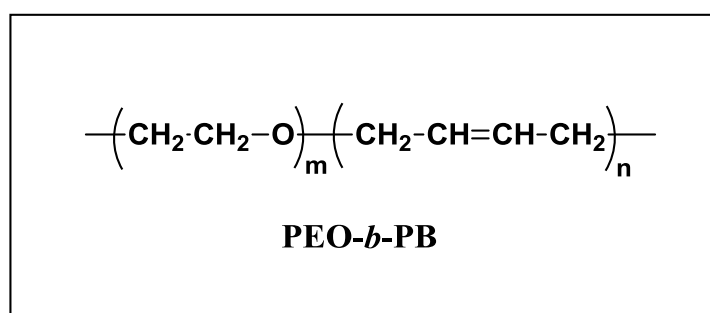


Figure 4. Structure formula of PEO-*b*-PB. The repeat unit of  $m$  is PEO block; the repeat unit of  $n$  is PB block.

Figure 5 displays the temperature-dependent SAXS profile of PEO<sub>7.5k</sub>-*b*-PB<sub>5.5k</sub> / h-PB<sub>1k</sub> blend with PEO volume fraction,  $f_{PEO} = 0.17$ . The system underwent a FCC-HCP OOT and an ODT from the HCP phase to disorder micelles in heating process, and then HCP showed up again in cooling process. FCC and HCP are composed of close-packing of equal sphere, but their stacking sequences are different, FCC is ABCABC-stacking, HCP is ABAB-stacking. I will choose two samples which the morphologies are FCC and HCP respectively to analyze their stacking sequences by TEMT. The FCC morphology is got from isothermal at 100°C; the HCP morphology is got from isothermal at 220°C

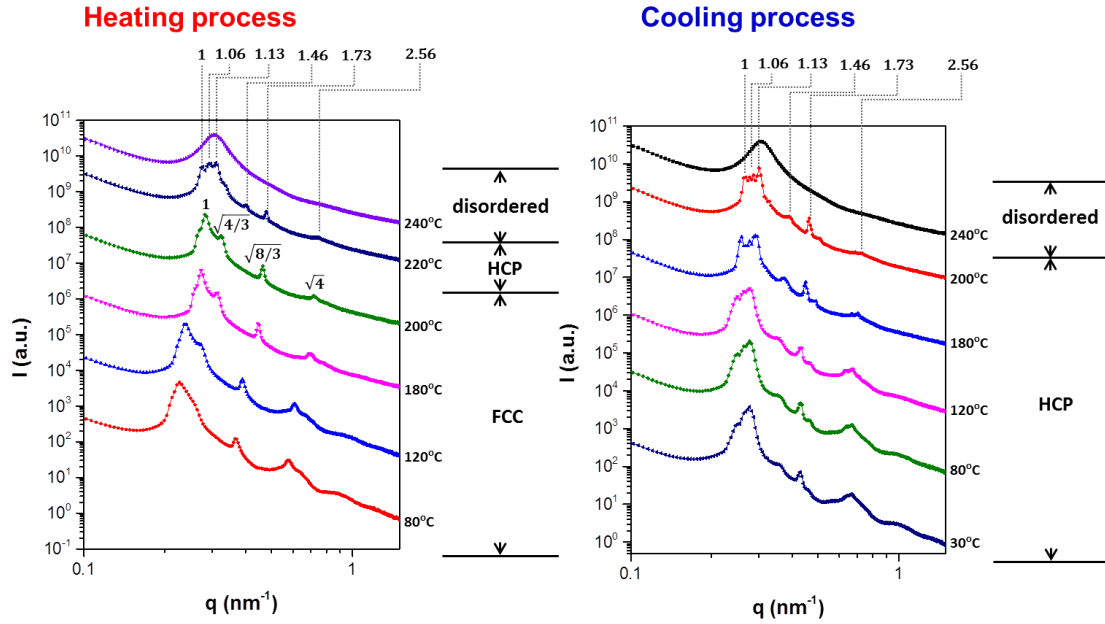


Figure 5. Temperature-dependent SAXS profile of PEO<sub>7.5k</sub>-*b*-PB<sub>5.5k</sub> / h-PB<sub>1k</sub> ( $f_{PEO} = 0.17$ ).

### (3) Sample preparation

#### (3a) Ultra-thin section

Because the glass transition temperature ( $T_g$ ) of ro254 and PEO<sub>7.5k</sub>-*b*-PB<sub>5.5k</sub> / h-PB<sub>1k</sub> ( $f_{PEO} = 0.17$ ) are below room temperature, they need to be sectioned by ultra-thin cryo-sectioning, the equipment is shown in Figure 6, the operational steps are as follows:

→ Setting: Transfer the sample to the cryo-chamber of an ultramicrotome which is cooled down to  $-40^\circ\text{C}$ .

→ Trimming: Set the cutting window for the sample. Use the trimming tool or a glass knife to face the block. This is to prepare a smooth reflective face to the block, from which the sections will be cut. The block is then squared to enable serial sections to come off as a ribbon. Use the reflective surface of the block to slowly bring the knife to the face of the block carefully without damaging the sample or the knife.

→ Sectioning: Ultrathin sections are cut at  $-40^\circ\text{C}$  to  $-50^\circ\text{C}$  for ro254,  $-100^\circ\text{C}$  for PEO<sub>7.5k</sub>-*b*-PB<sub>5.5k</sub> / h-PB<sub>1k</sub> ( $f_{PEO} = 0.17$ ); section thickness set to 50 nm ~ 70 nm. Using a hair (Dalmatian hair has a fine tip) to an area away from the knife edge. The sections are picked up using 2-3 mm loop containing a drop of 2.3M sucrose. The pick-up droplet should barely touch the surface of the knife for the sections to be captured. The loop is gently touched onto the surface of a coated grid to deposit the sections.

The samples are now ready for processing for direct imaging.



Figure 6. Ultra-thin cryo-sectioning equipment.

### (3b) Staining

TEM samples of polymers need high atomic number stains to enhance contrast. The stain absorbs the beam electrons or scatters part of the electron beam which otherwise is projected onto the imaging system. Compounds of heavy metals may be used prior to TEM observation to selectively deposit electron dense atoms in or on the sample in desired region. These stains are: osmium tetroxide ( $\text{OsO}_4$ ) for chemical unsaturation; ruthenium tetroxide ( $\text{RuO}_4$ ) for styrenics; and phosphotungstic acid for polyamides. *ro254* don't need to stain because it contains Si which is one of the electron dense atoms;  $\text{PEO}_{7.5\text{k}}\text{-}b\text{-PB}_{5.5\text{k}} / \text{h-PB}_{1\text{k}}$  ( $f_{\text{PEO}} = 0.17$ ) is need to be stained by  $\text{OsO}_4$ . Figure 7 shows the staining equipment. Before sectioning, bulk sample of  $\text{PEO}_{7.5\text{k}}\text{-}b\text{-PB}_{5.5\text{k}} / \text{h-PB}_{1\text{k}}$  ( $f_{\text{PEO}} = 0.17$ ) was stained by  $\text{OsO}_4$  for 32 hours at 1000 Pa, after sectioning, the film was stained again for 1 hours at 1000 Pa.



Figure 7. Staining equipment.

### (3c) Carbon coating

Figure 8 shows the carbon coating equipment. In order to avoid beam damage when conduct TEMT experiment, the sample need to do carbon coating after staining.



Figure 8. Carbon coating equipment.

### (4) Image collection

A JEOL JEM-2200FS model TEM (Figure 9) at an acceleration voltage of 200 kV was used to characterize the tomography images of the nanostructures. For the TEMT measurements, gold nanoparticles were placed on the backsides of the copper grids as the fiducial markers and a series of TEM images were obtained from  $70^\circ$  to  $-70^\circ$  at an angular

interval of  $1^\circ$ . Apply the software of “Recorder” to acquire highly accurate sequential tilted images required for 3D reconstruction of TEM images series automatically.



Figure 9. JEOL JEM-2200FS

#### (5) Image analysis

##### (5a) 3D reconstruction- Alignment of the data stack

Apply the software of “Composer” to reconstruct 3D images based on tilted images taken sequentially with a transmission electron microscope. The steps for reconstruction 3D images are summarized into five simple groups. It is possible to align and reconstruct (FBP/SIRT) 3D images quickly and simply.

##### (5b) 3D visualization

Apply the software of “Amira” to conduct 3D data visualization, analysis and modeling.

### **Results and discussion**

#### (1) The test sample (ro254)

At first we checked the morphology of ro254 which is quenched from  $200^\circ\text{C}$  from TEM micrograph, the image shown the domain is about 10 nm, this value is identical with SAXS data; the structures are the mix of lamellae and unknown structure (Figure 10).

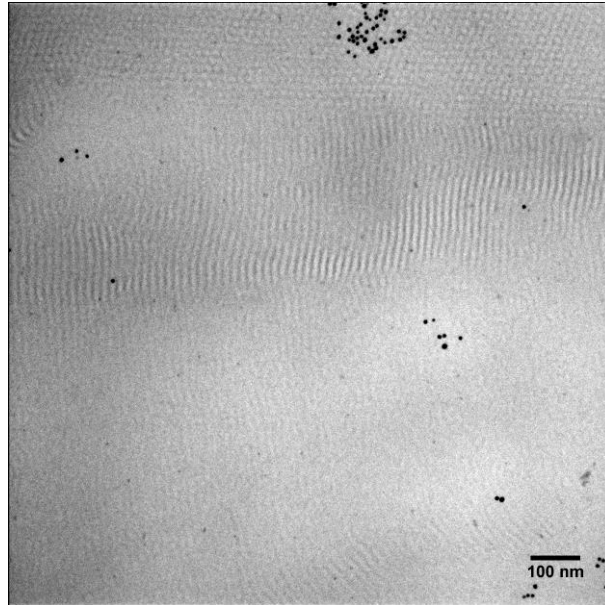


Figure 10. TEM micrograph of ro254.

Next, we reconstructed 3D images based on tilted images taken sequentially with a transmission electron microscope and apply SIRT calculated method for lamellae and unknown structure, respectively. The acquired images shown that the morphology is lamellae (Figure 11) and gyroid (Figure 12).

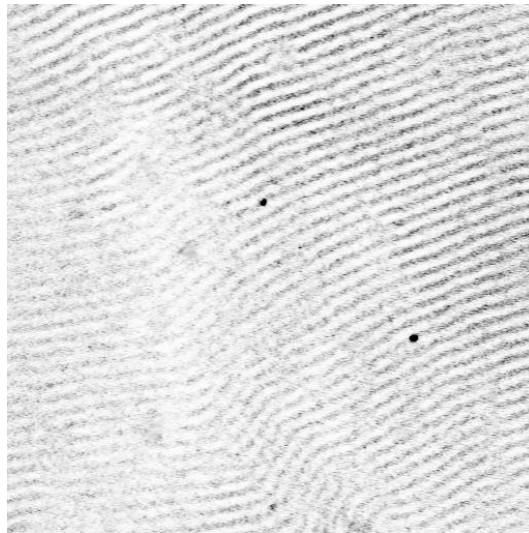


Figure 11. ro254 3D image reconstruct by SIRT. The structure is lamellae.

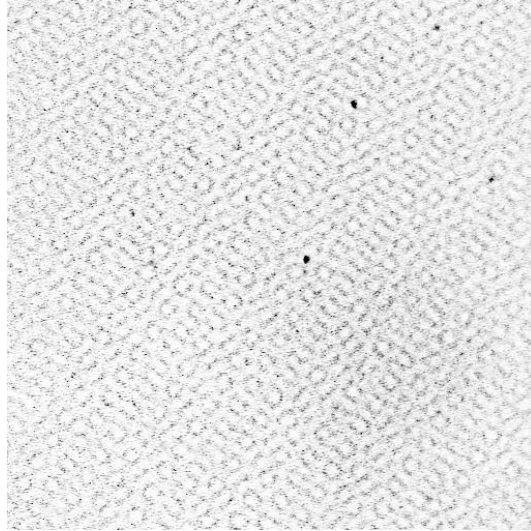


Figure 12. ro254 3D image reconstruct by SIRT. The structure is gyroid.

Finally, we conducted 3D image building and obtained rough 3D models of lamellae (Figure 13) and gyroid (Figure 14). Since the accuracy of 3D models considerably depends on the 3D image contrast, These models need to be decorated further.

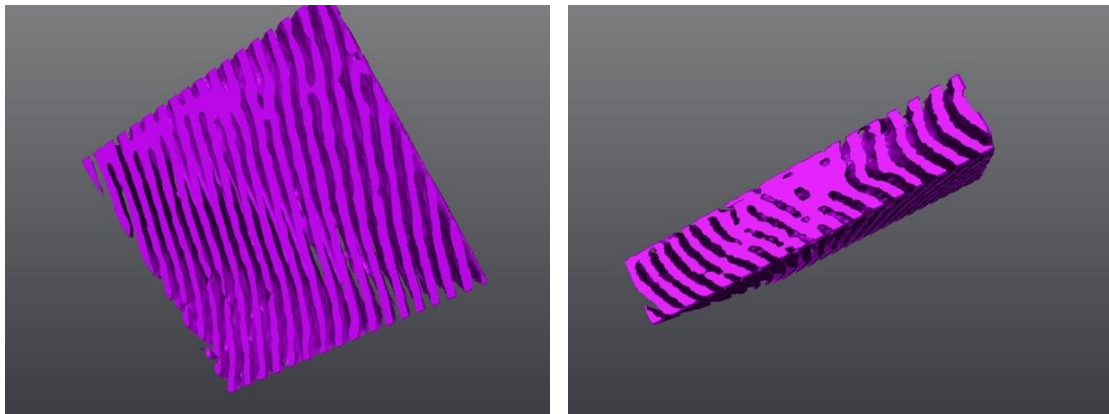


Figure 13. ro254 3D image building (a) xy plane; (b) xz plane. The structure is lamellae.

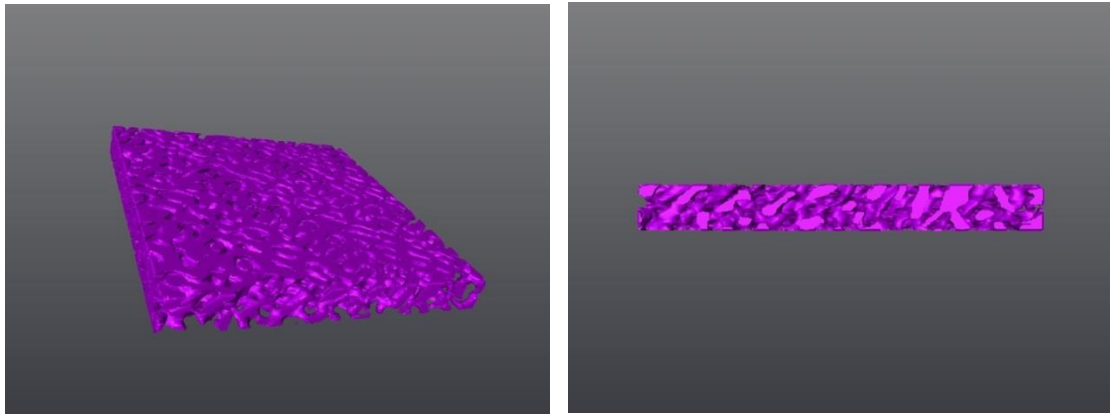


Figure 14. ro254 3D image building (a) xy plane; (b) xz plane. The structure is gyroid.

(2)  $\text{PEO}_{7.5\text{k}}\text{-}b\text{-PB}_{5.5\text{k}} / \text{h-PB}_{1\text{k}}$  ( $f_{\text{PEO}} = 0.17$ )

After tilt-series images collection, the sample suffered beam damage severely (Figure 15). Because of the beam damage and low contrast, the result of the reconstruction was not good, we couldn't do further analysis.

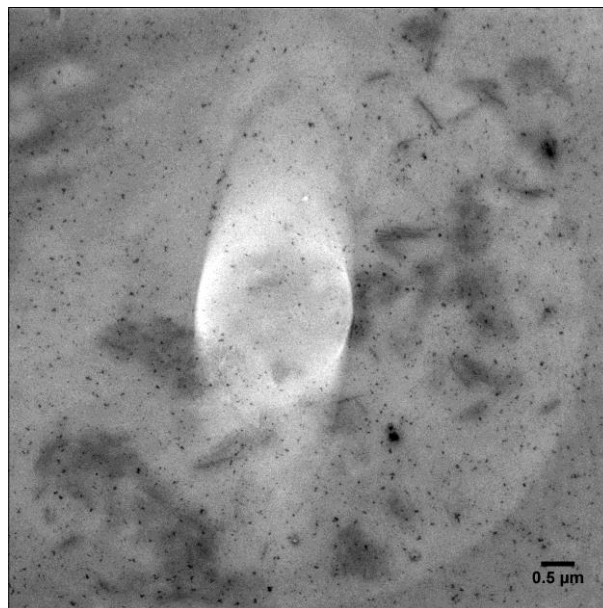


Figure 15. The scheme of beam damage (white region).

In order to protect sample against beam damage and improve image contrast, we tried to increase  $\text{OsO}_4$  staining pressure and staining time (pressure: 1000 Pa, time: 1 hour) and do carbon coating. When the staining pressures increased from 500 Pa to 1000 Pa, the contrast of images were improved, but the problem of beam damage still existed in the process of tilt-series images collection (Figure 16), we still couldn't collect suitable tilt-series images to conduct 3D image building.

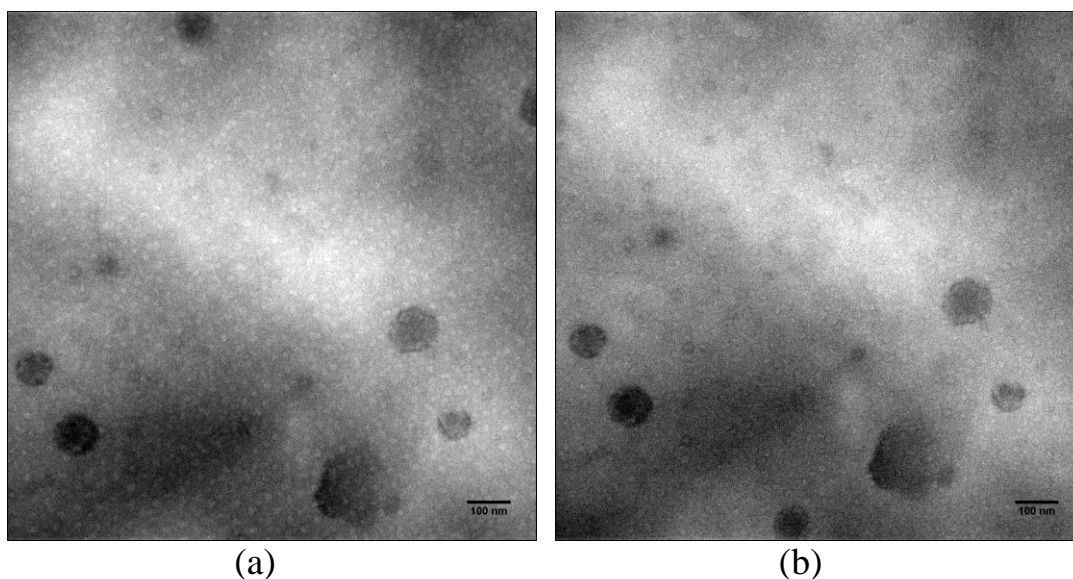


Figure 16. Sample no.1 OsO<sub>4</sub> staining (pressure: 1000 Pa, time: 1 hour) and carbon coating (a) before tilt-series images collection; (b) after tilt-series images collection

## Conclusions

TEM is an important measurement to visualize polymeric microstructure and can make up for the shortage of SAXS. In order to acquire the best 3D model, the quality of image contrast is very important. However, the system of PEO<sub>7.5k</sub>-*b*-PB<sub>5.5k</sub> / h-PB<sub>1k</sub> ( $f_{PEO} = 0.17$ ) suffered beam damaged severely in the process of tomography, we couldn't reconstruct the 3D model to analyze the stacking sequence. We'll take advantage of cryo-tomography in the future if there is a chance to cooperate with each other.

**Acknowledgment.** I gratefully acknowledge financial support from the Japan - Taiwan Exchange Association.

## References

1. Leibler, L. *Macromolecules* 1980, 13, 1602.
2. Hashimoto, T.; Shibayama, M.; Fujimura, M.; Kawai, H. In *Block Copolymers Science and Technology*; Meier, D. J., Ed.; Harward Academic Publishers: London, 1983.
3. Bates, F. S.; Fredrickson, G. H. *Phys. Today* 1999, 52, 32.
4. Matsen, M. W.; Bates, F. S. *Macromolecules* 1996, 29, 1091.
5. Matsen, M. W., 1995, 28, 5765-5773.
6. Matsen, M. W., *Physical Review Letters*, 1995, 74, 4225-4228.
7. Huang, Y. -Y; Chen, H. -L; Hashimoto, T., 2003, 36, 764-770.
8. Huang, Y. -Y; Hsu, J. -Y; Chen, H. -L; Hashimoto, T., 2007, 40, 3700-3707.